Proc. 1996 Int. Conf. on Plasma Physics,
Nagoya, 1996

Simulation of the MHD Kelvin-Helmholtz instability including vortex pairing: tangential stress at the magnetospheric boundary

Akira Miura

Department of Earth and Planetary Physics

University of Tokyo , Bunkyo-ku, Tokyo 113 Japan

Abstract

Magnetohydrodynamic (MHD) simulations of the Kelvin-Helmholtz (K-H) instability driven by the velocity shear in a 2-D plane perpendicular to the magnetic field show that after the nonlinear saturation of the linearly fastest growing vortices, the vortex train formed by the K-H instability is further susceptible to the vortex pairing, which continues as long as the length of the simulation system allows it. Each vortex formed in the fast rarefaction region is associated with an eddy current, which is inertia current in nature. The net momentum transport and shear relaxation by the instability occur as long as the vortex pairing continues. The momentum transport resulting in a velocity shear relaxation by the vortex pairing is much larger than that due to the growth of the fastest growing mode. A large tangential stress is imposed on the magnetopause by the K-H instability and is responsible for a tailward stretching of geomagnetic field lines.

The K-H instability is important in understanding a variety of phenomena involving sheared plasma flow in space [1,2] and astrophysical [3] phenomena. Space observations in situ have shown that the instability occurs at the earth's magnetopause and they have suggested a close connection between the magnetopause K-H instability and the existence of a flow boundary layer within the magnetopause [4]. The complete understanding of the $\mathbf{E} \times \mathbf{B}$ shear stabilization and/or destabilization of turbulence at the plasma boundary may also be important in improving plasma confinement in tokamak and stellarator plasmas. Hydrodynamical experiments have shown that at the late stage of the K-H instability, two vortical structures combine to form a single, larger vortical structure [5]. Such vortex pairing in the K-H instability has been reproduced by numerical experiments of the 2-D hydrodynamics [6] and 2-D magnetohydrodynamics [2]. The purpose of this paper is to understand the basic relationship among vortex development, fast rarefaction, eddy current, and momentum transport by the instability in a 2-D plane transverse to the magnetic field by using an MHD simulation. The previous 2-D MHD simulations [2] done for different configurations including a flow parallel to the magnetic field have not addressed the basic relationship.

MHD simulations are performed in the $x - y$ plane perpendicular to the magnetic field, where the initial flow velocity v_{0y} has a shear profile $v_{0y}(x) = V_0/2\ (1 - \tanh(x/a))$ and the other equilibrium quantities are uniform. In this configuration, the wavelength of the fastest growing mode λ_{FGM} is equal to 15.7a and its growth rate is equal to $0.13V_0/2a$ [7]. The length L_y of the simulation system is equal to $4 \cdot \lambda_{FGM} = 62.8a$. At T=0, a superposition of the linear eigenfunction of the fastest growing mode and its subharmonic modes is added to the equilibrium as an initial perturbation with a small amplitude. When the plasma is compressible and $\gamma \neq 2$ as in the present simulation ($\gamma = 5/3$ is the ratio of specific heats), **B** appears explicitly in the governing equations and there is essential difference of the K-H instability between the 2-D transverse MHD case ($\partial/\partial z = 0$) and the 2-D hydrodynamic case. In the 2-D incompressible, inviscid hydrodynamic flow the total kinetic energy and the mean enstrophy (square vorticity) must remain constant during the fluid motion [8]. This fact imposes a requirement in the 2-D hydrodynamics that the bulk of the energy concentrates in the small wave-number; in other words the fluid elements with similarly signed vorticity must tend to group together [8]. In the 2-D MHD transverse case, we obtain

$$\frac{\partial}{\partial t}\int dxdy\,(\nabla\times\mathbf{v})^2 = -\int dxdy(\nabla\times\mathbf{v})^2\nabla\cdot\mathbf{v} + 2\int dxdy(\nabla\times\mathbf{v})\cdot\left(\frac{\nabla\rho}{\rho}\times\frac{\nabla p_t}{\rho}\right).$$

Therefore, when $\nabla\cdot\mathbf{v} = 0$ and $\nabla\rho$ is parallel to ∇p_t, where p_t is the total pressure defined by $p_t = p + B^2/2\mu_0$, the mean enstrophy must be conserved. This means that the same tendency for the bulk of energy to concentrate in the small wave-numbers is also expected for a 2-D MHD transverse case, where the compressibility is small and $\nabla\rho$ is parallel to ∇p_t.

Figure 1 shows contour lines of the z-component of the vorticity at eight different times. The contour lines are plotted for negative vorticity. In the early phase four vortices appear as predicted by the linear theory. At T= 80 two vortices are formed out of the initial four

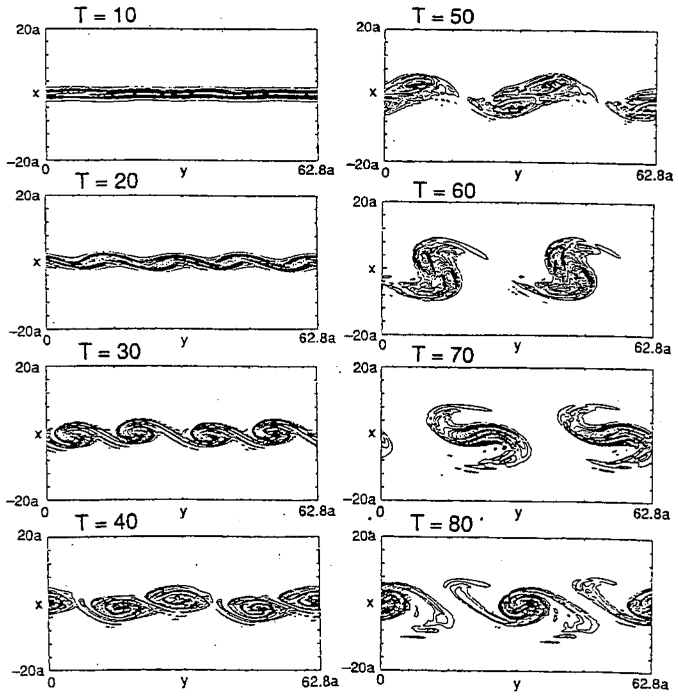

Fig. 1. Contour lines of the z-component of the vorticity at eight different times.

vortices. This process of the vortex pairing is very similar to that reported in the hydrodynamics [5,6].

Figure 2 shows contour lines of pressure (top), flow velocity vectors (middle), and current vectors (bottom) at two different times. By T= 40 (left panels) four pairs of high pressure (compressed) region and low pressure (rarefied) region have lined up near x~0. At the peak of the high pressure region (denoted by H), the peak pressure reaches $1.14p_0$, where p_0 is the initial uniform pressure. At the bottom of the low pressure region (denoted by L) the pressure becomes $0.776p_0$. The rarefied region has a much steeper pressure gradient than in the compressed region. The middle left panel shows that four flow vortices have developed near x = 0 in the rarefied region by T=40. The bottom left panel shows that the eddy current is associated with each flow vortex. The eddy current in the rarefied region is the inertia current in nature. In other words, the centrifugal force by the vortical rotation is balanced by the $\mathbf{J} \times \mathbf{B}$ force directed to the center of the vortex. The top right panel shows that a pair of low and high pressure regions develops after the second vortex pairing at T = 230. In the low pressure region the minimum pressure becomes as low as $0.481p_0$ owing to a strong fast rarefaction. In the rarefied region a large vortex develops. This panel also shows that in the compressed region, the large flow momentum in the y direction in x < 0 is transported to x > 0.

Figure 3 shows, from the top, profiles at T = 20 (left) and T=220 (right) across x of the normalized Reynolds stress, the x component of the normalized electric field $\langle E_x \rangle$, which is responsible for the $\mathbf{E} \times \mathbf{B}$ drift in the y direction, the normalized flow momentum profile

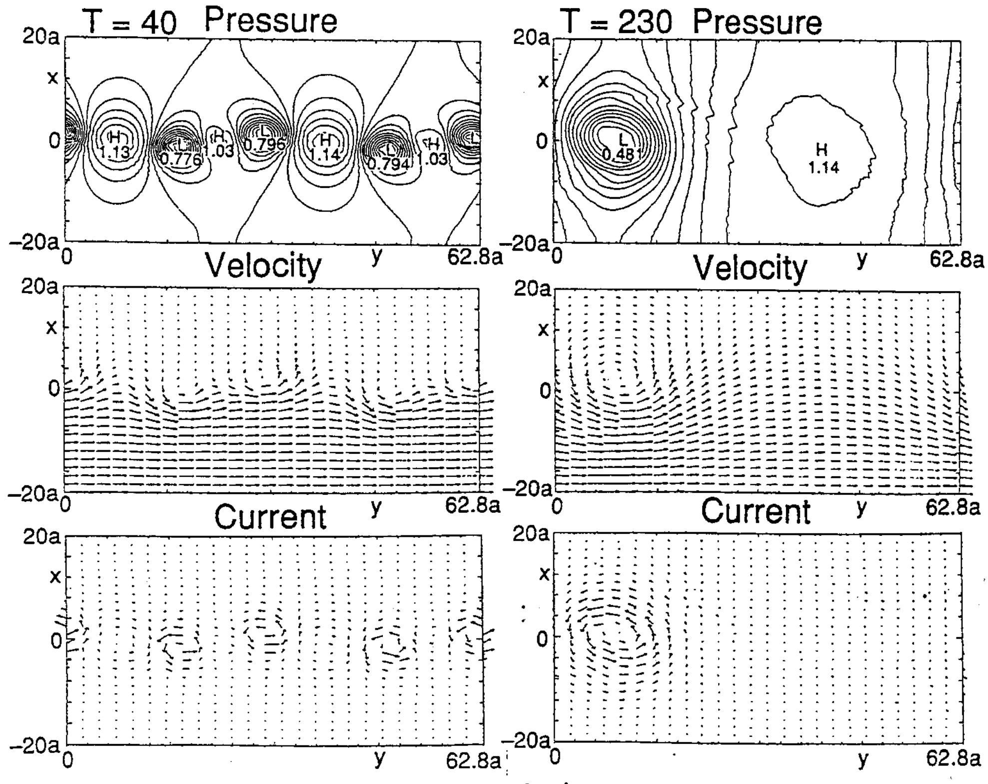

Fig. 2. Contour lines of pressure (top), flow velocity vectors (middle), and current vectors (bottom) at two different times T=40 (left) and T=230 (right).

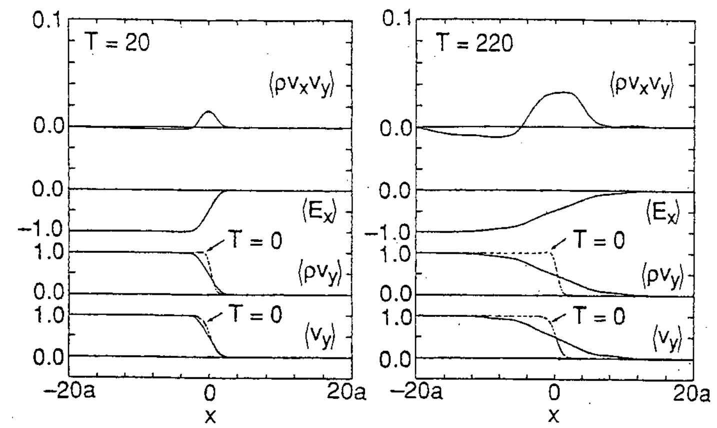

Fig. 3. Profiles at T = 20 (left) and T=220 (right) across x of the averaged Reynolds stress, the x component of the averaged electric field $<E_x>$, the averaged flow momentum $<\rho v_y>$, and the averaged flow velocity $<v_y>$ from the top. The dotted profiles show their initial profiles.

$<\rho v_y>$, and the normalized flow velocity profile $<v_y>$. The dotted profiles in $<\rho v_y>$ and $<v_y>$ show their initial profiles. Although the net momentum is transported from $x < 0$ to $x > 0$ by the growth of the fastest growing mode at T=20, much larger flow momentum is transported across x=0 by the coalescence of the fastest growing modes at T = 220.

In space and astrophysical applications the spatial growth of the K-H instability is more common than the temporal growth as treated here. Therefore, the large momentum transport by the vortex pairing is expected in the downstream region of the sheared plasma flow in space and astrophysics, e.g., at the downstream magnetopause.

References

[1] A. Miura, Phys. Rev. Lett. **49**, 779 (1982); A. Miura, J. Geophys. Res. **89**, 801 (1984); A. Miura, J. Geophys. Res. **97**, 10655 (1992); A. Miura, in *Physics of the Magnetopause* edited by P. Song, B.U.Ö. Sonnerup, and M.F. Thomsen, (American Geophysical Union, Washington, DC, 1995), p. 285.

[2] C.C. Wu, J. Geophys. Res. **91**, 3042 (1986); G. Belmont and G. Chanteur, Phys. Scr. **40**, 124 (1989); J.R. Manuel and J.C. Samson, J. Geophys. Res. **98**, 17367 (1993).

[3] D. Ryu, T.W. Jones, and A. Frank, Astrophys. J. **452**, 785 (1995); A. Malagoli, G. Bodo, and R. Rosner, Astrophys. J. **456**, 708 (1996); A. Frank et al., Astrophys. J. **460**, 777 (1996).

[4] S.-H. Chen et al., J. Geophys. Res. **98**, 5727 (1993); J. Seon et al., J. Geophys. Res. **100**, 11907 (1995).

[5] C. D. Winant and F.K. Browand, J. Fluid Mech. **63**, 237 (1974).

[6] G.M. Corcos and F.S. Sherman, J. Fluid Mech. **139**, 29 (1984).

[7] A. Miura and P.L. Pritchett, J. Geophys. Res. **87**, 7431 (1982).

[8] L. Onsager, Nuovo Cimento Suppl. **6**, 279 (1949).